PHYSICAL REVIEW E **66**, 055203(R) (2002)

Patterns in spherical Rayleigh-Bénard convection: A giant spiral roll and its dislocations

Pu Zhang
School of Mathematical Sciences, University of Exeter, Exeter EX4 4QE, United Kingdom

Xinhao Liao
Shanghai Astronomical Observatory, Shanghai 200030, China

Keke Zhang*
School of Mathematical Sciences, University of Exeter, Exeter EX4 4QE, United Kingdom
(Received 5 June 2002; published 21 November 2002)

Thermal convection in a moderately thin spherical fluid layer in the presence of spherically symmetric gravity, spherical Rayleigh-Bénard convection, is investigated through fully three-dimensional numerical simulations. A steady spherical pattern in the form of a single giant spiral roll covering the whole spherical surface without defects is discovered near the onset of convection. Successive dislocations of the giant spiral roll are also found at larger Rayleigh numbers.

DOI: 10.1103/PhysRevE.66.055203 PACS number(s): 47.54.+r, 47.27.Te, 92.60.Ek

Thermal convection in a spherical fluid layer subject to a spherically symmetric radial gravity force and a spherically symmetric boundary condition, which will be referred to as spherical Rayleigh-Bénard convection, is associated with many natural phenomena in geophysical and astrophysical fluid systems [1–3]. Spherical Rayleigh-Bénard convection also represents an extensively studied exemplary fluid system involving the pattern and orientational degeneracies [4–8]. This paper reports a steady pattern discovered in spherical Rayleigh-Bénard convection: a single, perfect, giant spherical spiral roll extending all the way from the north pole to the south pole and its successive dislocations.

We consider a Boussinesq fluid of uniform viscosity ν confined in a spherical layer bounded by two concentric spherical surfaces of inner radius r_i and outer radius r_o which have nonslip velocity and isothermal temperature boundary conditions. Fluid motions in the spherical fluid layer are driven by a spherically symmetric gravity force in connection with a spherically symmetric distribution of heat sources, a well-known spherical convection model proposed by Chandrasekhar [9]. There are three dimensionless control parameters in spherical Rayleigh-Bénard convection: geometrical aspect ratio $\eta=2\pi r_o/(r_o-r_i)$, the Rayleigh number R, and the Prandtl number Pr.

In the limit of large aspect ratio $\eta\to\infty$, the mathematical problem of spherical Rayleigh-Bénard convection becomes identical to that of the classical Rayleigh-Bénard convection in an infinitely extended horizontal fluid layer heated from below. The plane-layer Rayleigh-Bénard convection is perhaps the most intensively studied nonlinear system in the understanding of its pattern formation [10–14]. Thermal convection occurs when the Rayleigh number R reaches its critical value $R_c=1708$. Near the onset of convection, roll, triangular, hexagonal, and square patterns can exist. In a number of well-controlled experiments in a cylindrical container of large aspect ratio 86 using a non-Boussinesq fluid, Bodenschatz, de Bruyn, and Cannel in Ref. [15] (see also [16]) found giant stable rotating spirals, with a number of dislocations, extending from the spiral core to the boundary of the cylindrical container. The spiral rotates such that the resulting waves propagate radially outward from the core.

When aspect ratio η is finite, the effect of spherical geometry plays an essential role and the selection of nonlinear pattern bifurcating from a spherical symmetric basic state poses a complicated and difficult problem [5,6]. At the onset of spherical Rayleigh-Bénard convection, $R=R_c$, the general linear solution may be written, for example, as

$$u_r=f_l(r)\sum_{m=0}^{m=l}(C_m\cos m\phi+S_m\sin m\phi)P_l^m(\cos\theta), \quad (1)$$

where (r,θ,ϕ) are spherical polar coordinates, u_r is the radial flow, $f_l(r)$ represents a radial eigenfunction, $P_l^m(\cos\theta)$ denotes standard spherical harmonics of degree l and $C_m, S_m, m=0,1,\ldots,l$ are $(2l+1)$ arbitrary constants. The value of l corresponds to the minimum Rayleigh number required to initiate convection. Equation (1) indicates that there exists the $(2l+1)$ fold degeneracy of the solution. A complete elimination of the $(2l+1)$ fold degeneracy by nonlinearity proves to be a mathematically challenging task. Busse [5] (see also Ref. [8]) showed that the solvability conditions for the weakly nonlinear problem with $2\leqslant l\leqslant 6$ select a small number of steady convection patterns (there is no pattern degeneracy for the special cases with $l=0$ and $l=1$). He also showed that the solvability condition at the third-order perturbation is independent of the radial dependence of the problem. Consequently, the possible patterns can be determined without the actual knowledge of radial functions like $f_l(r)$ in Eq. (1). The further stability analysis suggests that, for example, the axisymmetric solution is preferred for $l=2$ and the tetrahedral solution is stable for $l=3$. It is important, however, to note that an assumption that all solutions of the nonlinear problem possess symmetry with respect to a plane through the center of the sphere is made to

*Electronic address: KZhang@ex.ac.uk

simplify the mathematical analysis. By taking the plane at $\phi=0$, the assumption of the plane symmetry leads to

$$S_m=0, \quad m=1,\ldots,l, \tag{2}$$

in Eq. (1). In consequence, the $(2l+1)$ fold degeneracy of the solution is reduced to the $(l+1)$ fold degeneracy.

The value of l for the onset of spherical Rayleigh-Bénard convection is solely determined by the size of aspect ratio η. For a thick spherical fluid layer with $l=O(1)$, the convection problem has been studied explicitly [5,8] (see also the group theoretical method by Chossat in Ref. [6]). Thermal convection in a thin spherical layer with $l>6$, which is more complicated and of no less mathematical and physical interest, has not been investigated in detail. We study nonlinear spherical Rayleigh-Bénard convection using fully three-dimensional numerical simulations in a spherical layer with aspect ratio $\eta=41.2$. Our linear analysis, which is independent of nonlinear simulations of the convection problem, shows that

$$R(l=17)=1723.5, \quad R(l=18)=1710.7,$$

$$R(l=19)=1712.4, \quad R(l=20)=1727.1.$$

The critical Rayleigh number for the onset of convection at $\eta=41.2$ is given by $R_c=1710.7$ with $l=18$, which is slightly larger than that for the plane-layer Rayleigh-Bénard convection $R_c=1708$ at $\eta\to\infty$. It follows that the solution at the bifurcation point has the 37-fold degeneracy. It should be noted that the value of $R(l=19)$ is only slightly larger than the critical one.

Our numerical simulation starts with an initial condition involving an azimuthal wave number $m=1$ near the onset of convection for $\epsilon=(R/R_c)-1=0.28$ and Pr=7.0. Numerically speaking, it is difficult as well as impractical to simulate convection directly in the neighborhood of bifurcation for $\epsilon\ll 1$ since it takes an extremely long time to reach a steady equilibrium. Our convection simulation for moderate $\epsilon=0.28$ takes about 20 t_ν, where t_ν is the viscous diffusion time $(r_o-r_i)^2/\nu$, to reach a steady equilibrium. The total simulation for this case lasted about $32t_\nu$. From $20t_\nu$ to $32t_\nu$, the simulated convection remains unchanged both temporally and spatially. The steady equilibrium is described by a single, giant spiral roll extending from the north pole to the south pole without defects and covering the whole spherical surface, which is shown in Fig. 1. Of course, the position of the pole at which the spiral roll starts or ends is arbitrary because of orientational degeneracy. Furthermore, as we should expect, the spiral roll is not the only stable pattern at the parameters of the problem. Different initial conditions usually lead to different convection patterns such as the symmetric ones with $S_m=0$.

Using the exactly same initial condition, we also simulate spherical Rayleigh-Bénard convection for a number of larger Rayleigh numbers. It is found that the final equilibrium of nonlinear convection at $\epsilon=1.57$ is also stationary. However, the giant spiral roll is no longer perfect and three dislocations take place in the northern hemisphere and the equatorial region, which is depicted in Fig. 2. As nonlinear effects increase further to $\epsilon=3.28$, the final steady equilibrium of our simulation using the same initial condition, displayed in Fig. 3, exhibits more dislocations in both the southern and northern hemispheres concentrating in lower latitudes where the nonlinear stresses are likely to be largest.

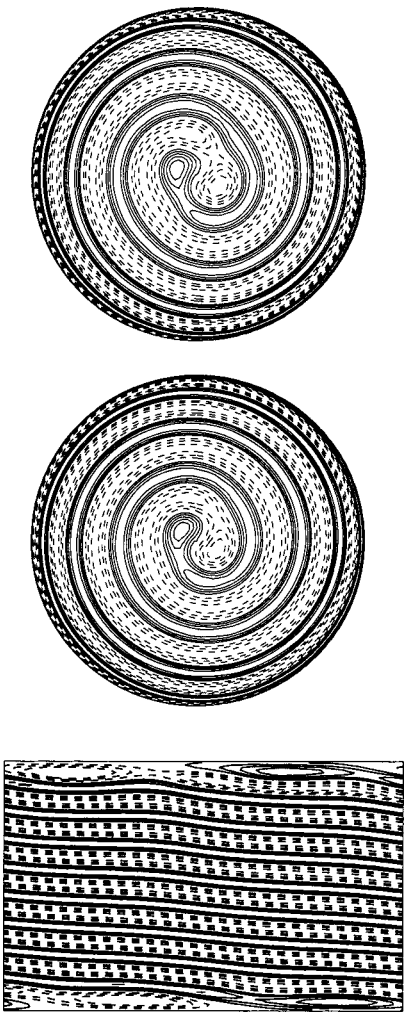

FIG. 1. Contours of radial flow u_r at the middle surface of the spherical shell for $\epsilon=(R/R_c)-1=0.28(R_c=1710.7)$ and Pr=7.0. Dashed contours indicate radially inward flow $u_r<0$ and solid contours correspond to radially outward flow $u_r>0$. The top (middle) panel shows the contours viewed from the north (south) pole. To display the equatorial region clearly, the lower panel shows the projection of the middle spherical surface onto a rectangular domain.

We have found a single, giant, perfect spiral roll in the problem of spherical Rayleigh-Bénard convection. It is of interest to compare the spherical spiral with the cylindrical spiral. The spiral in a cylindrical container is time dependent in the form of radially traveling waves with a non-Boussinesq fluid [15]. A sidewall forcing appears to be needed to prevent it from drifting toward the sidewall in the case of the cylindrical spiral [14,16]. Decker, Pesch, and Weber [17] also simulated spiral rolls with a Boussinesq fluid for large aspect ratio systems using a Galerkin method. Our giant spherical spiral roll is stationary and can be regarded as two individual hemispherical spiral rolls that merge at the

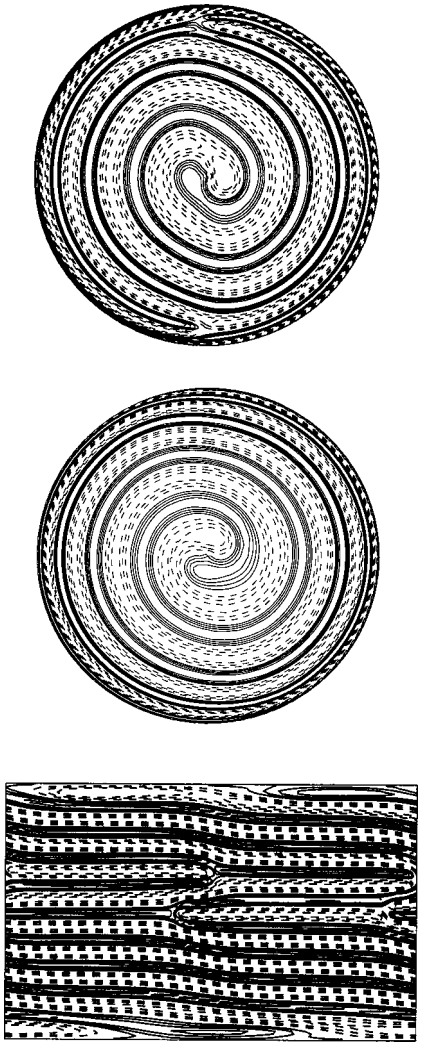

FIG. 2. The same as Fig. 1, except for $\epsilon = 1.57$.

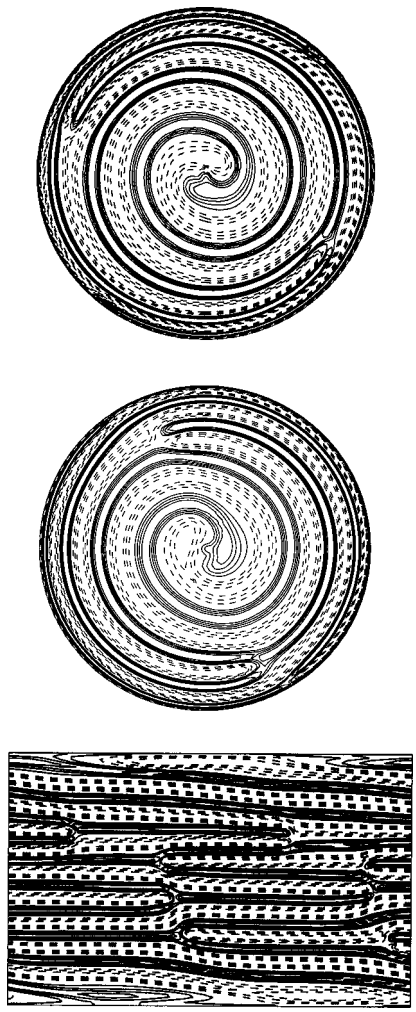

FIG. 3. The same as Fig. 1, except for $\epsilon = 3.28$.

equator, a consequence of specific topology of the spherical-geometry convection roll. In other words, it is spherical geometry that naturally guides a single giant spiral roll circuiting the whole spherical surface like a long snake.

The discovery of the giant spherical spiral roll suggests the importance of plane asymmetric coefficients S_m in Eq. (1). In fact, the plane symmetry assumption given by Eq. (2) excludes the possibility of convection pattern in the form of a single giant spherical spiral roll shown in Fig. 1. The linear analysis indicates that the giant spiral pattern is a result of a mixed-mode bifurcation involving P_{18}^1 and P_{19}^1. Because of the difficulties in simulating numerically three-dimensional, thin-shell spherical convection near the bifurcation point, a perturbation analysis would be much more appropriate for a weakly nonlinear problem. An extension of Busse's perturbation analysis to include the nonzero coefficients S_m and a detailed study of the dependence of the spiral spherical convection on the Prandtl number is currently underway and will be reported in a future paper.

ACKNOWLEDGMENTS

We are grateful to F. H. Busse, P. Matthews, and M. Proctor for helpful discussions. P.Z. is supported by UK ORS and X.L. is supported by NSFC and MOST grants.

[1] G. Schubert, Annu. Rev. Fluid Mech. **7**, 289 (1979).
[2] K. Zhang and F.H. Busse, Phys. Earth Planet. Inter. **104**, 283 (1997).
[3] K. Zhang and F.H. Busse, Adv. Fluid Mechanics **20**, 17 (1997).
[4] R.E. Young, J. Fluid Mech. **63**, 695 (1974).
[5] F.H. Busse, J. Fluid Mech. **72**, 67 (1975).
[6] P. Chossat, SIAM (Soc. Ind. Appl. Math.) J. Appl. Math. **37**, 627 (1979).
[7] G. Schubert and A. Zebib, Geophys. Astrophys. Fluid Dyn. **15**, 65 (1980).
[8] F.H. Busse and N. Riahi, J. Fluid Mech. **123**, 283 (1982).
[9] S. Chandrasekhar, *Hydrodynamic and Hydromagnetic Stability* (Clarendon Press, Oxford, 1961).
[10] G. Veronis, J. Fluid Mech. **5**, 410 (1959).

[11] L.A. Segel, J. Fluid Mech. **38**, 203 (1969).
[12] F.H. Busse, Rep. Prog. Phys. **41**, 1929 (1978).
[13] M.C. Cross and P.C. Hohenberg, Rev. Mod. Phys. **65**, 851 (1993).
[14] E. Bodenschatz, Annu. Rev. Fluid Mech. **32**, 709 (2000).
[15] G.A.E. Bodenschatz, J.R. de Bruyn, and D.S. Cannell, Phys. Rev. Lett. **67**, 3078 (1991).
[16] B.B. Plapp and E. Bodenschatz, Phys. Scr., T **67**, 111 (1996).
[17] W.P.W. Decker, W. Pesch, and A. Weber, Phys. Rev. Lett. **73**, 648 (1994).